

Opinion Market Model: Stemming Far-Right Opinion Spread using Positive Interventions

Pio Calderon
piogabrielle.b.calderon@student.uts.edu.au
University of Technology Sydney
Sydney, Australia

Rohit Ram
rohit.ram@uts.edu.au
University of Technology Sydney
Sydney, Australia

Marian-Andrei Rizoiu
marian-andrei.rizoiu@uts.edu.au
University of Technology Sydney
Sydney, Australia

ABSTRACT

Recent years have seen the rise of extremist views in the opinion ecosystem we call social media. Allowing online extremism to persist has dire societal consequences, and efforts to mitigate it are continuously explored. Positive interventions, controlled signals that add attention to the opinion ecosystem with the aim of boosting certain opinions, are one such pathway for mitigation. This work proposes a platform to test the effectiveness of positive interventions, through the Opinion Market Model (OMM), a two-tier model of the online opinion ecosystem jointly accounting for both inter-opinion interactions and the role of positive interventions. The first tier models the size of the opinion attention market using the multivariate discrete-time Hawkes process; the second tier leverages the market share attraction model to model opinions cooperating and competing for market share given limited attention. On a synthetic dataset, we show the convergence of our proposed estimation scheme. On a dataset of Facebook and Twitter discussions containing moderate and far-right opinions about bushfires and climate change, we show superior predictive performance over the state-of-the-art and the ability to uncover latent opinion interactions. Lastly, we use OMM to demonstrate the effectiveness of mainstream media coverage as a positive intervention in suppressing far-right opinions.

1 INTRODUCTION

Online social media platforms are fertile grounds for deliberation and opinion formation [2, 13, 22, 34]. Opinions thrive in an *online opinion ecosystem*, where they interact – cooperate or compete for the finite public attention [40] – within and across online social groups. The opinion ecosystem also has a dark side. The rise of misinformation [19], filter bubbles and echo chambers [4, 11, 12, 15, 21, 33] have led to the rampancy of extremist worldviews [8, 37, 38], leading to detrimental societal consequences such as oppression [10, 27] and political violence [16].

We delineate two types of interventions to mitigate the spread of extremist views. *Negative interventions* aim to subtract attention from the opinion ecosystem by placing fact-check warnings on postings [26], shadowbanning [42] or outright banning extremist social media groups and accounts [20]. While negative interventions are effective [6], they are available solely to the social media platforms who tend to use them sparsely [28]. *Positive interventions*, such as misinformation debunking [14, 32, 39, 41] and increasing media coverage [18], mitigate extremist views by adding attention

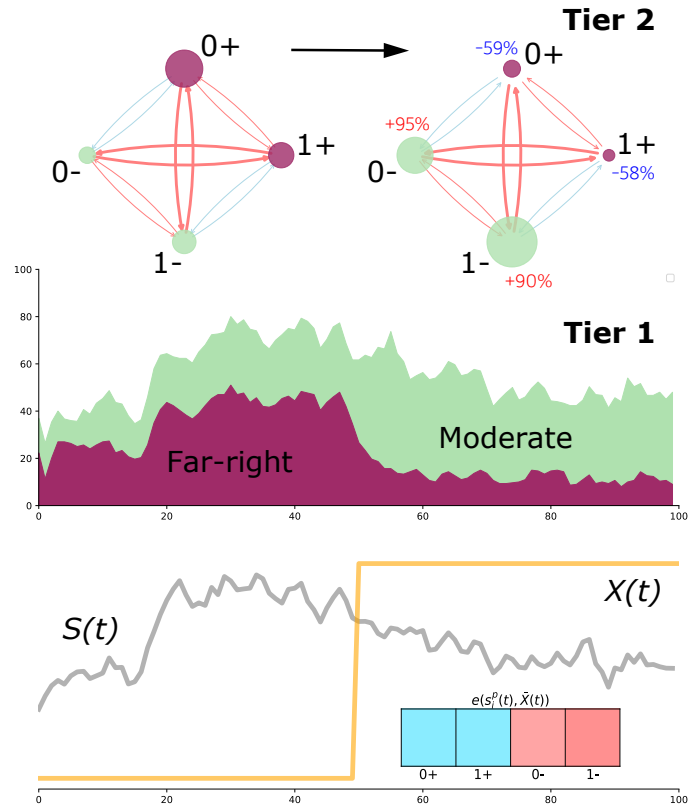


Figure 1: Suppressing far-right opinion with positive interventions. A simulated toy opinion ecosystem with two far-right (+) and two moderate (-) opinions. *Bottom row:* the exogenous signal $S(t)$ (defined in Eq. (7)) and intervention $X(t)$ (defined in Eq. (11)). We set $X(t)$ as a step function with change point $t = 50$. The inset shows the instantaneous reaction of the four opinions to the intervention (blue signifies inhibition and red is reinforcement). *Middle row:* Total daily opinion market size quantified by our model’s first tier, split into far-right (+) and moderate (-) opinion volumes. *Top row:* Market shares and the interactions between the four opinions estimated by our model’s second tier. Nodes are opinions; their sizes indicate market share; edges represent exciting (red) and inhibiting (blue) relations. $X(t)$ suppresses far-right opinions for $t > 50$. Shown are average market shares before (left) and after (right) $t = 50$.

to the online opinion ecosystem through informing the public, redistributing attention away from extremist, and toward moderate, views. Such interventions are typically in the hands of government and media agencies. Testing the viability of positive interventions requires capturing reactions to interventions and inter-opinion interactions.

This work develops a model for the dynamics of the opinion ecosystem and a test bed for evaluating positive interventions. We focus on two open questions. The first explores the analogy between opinions and economic goods. In a competitive economic market of limited resources, coexisting goods can interact in one of two ways: either they compete for market share (*substitute* brands, like Pepsi and Coke) or reinforce each other (*complementary* items, like bread and butter). We argue that opinions in the online ecosystem behave similarly, allowing us to leverage market share modeling tools [7]. The first research question is: **Can we model the online opinion ecosystem as an environment where opinions cooperate or compete for market share?** We propose the Opinion Market Model¹ (OMM), a two-tier model to solve this problem – showcased in Fig. 1, using a simple opinion ecosystem under intervention. We consider a single social media platform and two opinions (denoted 0 and 1). Each opinion has two polarities: that of far-right supporters (+) and that of moderate debunkers (-). The first tier of OMM (middle row in Fig. 1) uses a discrete-time Hawkes process to estimate the size of the opinion attention market – that is, the daily number of postings featuring opinions. The online opinion ecosystem is not a closed system; it contains exogenous signals and interventions. Exogenous signals such as natural (e.g., bushfires) or political (e.g., speeches, decisions) events modulate the size of the opinion ecosystem (shown in gray in the bottom panel of Fig. 1). Interventions act by adding attention to the opinion ecosystem, boosting and suppressing certain opinions (shown in yellow). The second tier of OMM (top row in Fig. 1) leverages a market share attraction model to capture opinion interactions. For the example in Fig. 1, opinions 0– and 1+ have a strong reinforcing relation (shown in red), while 1– and 1+ have a weak competing relation (blue).

We test OMM on a dataset of Facebook and Twitter discussions containing moderate and far-right opinions about bushfires and climate change [23]. OMM shows strong predictive and interpretation capabilities. We show it outperforms the current state of the art in product share modeling (Competing Products model [35]). It also exposes the relations between opinions on the two platforms. On Facebook, no significant interactions take place, as postings were collected from far-right public groups that have limited interaction with the opposing side. On Twitter, we observe the self-reinforcement behavior of both far-right and moderate opinions, probably due to the echo chamber effect [5]. Surprisingly, we also notice that opposing views reinforce each other, probably due to the deliberative nature of Twitter, where far-right opinion sympathisers and opponents oppose each other.

Our second research question is: **Can we test the sensitivity of the opinion ecosystem to positive interventions?** OMM accounts for positive interventions – controlled external signals aimed at boosting certain opinions. In Fig. 1 an intervention is performed for $t > 50$ which suppresses the far-right opinions (+),

leading to the shrinking of their market share. We use OMM for two tasks: to estimate whether interventions effectively shape the opinion ecosystem and construct what-if scenarios to test future interventions. For the bushfire case study, we test whether mainstream media coverage as an intervention allows the suppression of far-right opinions. We fit OMM twice to the far-right dataset for the first task: with and without mainstream media coverage. We find a better fit with the intervention, suggesting that mainstream media has an active role in shaping the opinion ecosystem. We perform synthetic what-if experiments: we modulate the intervention and run the system forward. We find that the market share of far-right opinions decreases as mainstream media coverage increases, showing the effectiveness of media coverage in stemming far-right content propagation. One notable exception was the opinion that "Mainstream media cannot be trusted," which was less responsive to the intervention.

The main contributions of the work are the following:

- (1) We introduce a two-tier model of the opinion ecosystem that exploits the analogy between opinions and economic goods, allowing opinion interactions to be studied through an economics-based cooperation-competition lens.
- (2) We introduce algorithms for simulation and estimation of the proposed two-tier model and demonstrate the convergence of our estimation scheme through synthetic tests.
- (3) We apply OMM to a dataset of Twitter and Facebook discussions related to bushfires and climate change, uncovering interactions across sympathizers and opponents of far-right opinions and showing how reputable media coverage acts as an intervention to suppress far-right opinions.

Related Work. A number of previous studies in information diffusion analysis have focused on modeling the cooperative-competitive interaction in a set of co-diffusing online items. The Clash of the Contagions model [25] frames interaction as the perturbation in the probability of *infection* (i.e., adoption) of a given *contagion* (i.e., online item), after exposure to a set of competing contagions. The InterRate model [29] approaches the task as a kernel estimation problem [44], inferring an *interaction profile* that characterizes the temporal evolution of the interaction effect. Closely related to this work is the Correlated Cascades model [43], a variant of the multivariate Hawkes model to model product adoption across a set of competing products in a social network. There they estimate the interaction parameter β , which tunes the level of cooperation or competition in the market. A limitation of this work is that a single β is shared across all products, which simplifies asymmetric relationships that exist and assumes that all brands either cooperate or compete. Our work models these asymmetric relationships fully. Another closely related work is the Competing Products (CP) model [35], a multivariate Hawkes model for product adoption and use where the frequency of use is affected by the usage of other products. A technical limitation of the work is that competitive interactions are modeled as negative parameters in the Hawkes intensity, leading to negative intensity values. OMM naturally avoids this weakness by modeling opinion shares as fractions of the total attention volume. The SLANT model [9] is a model of opinion dynamics with close ties to the CP model. It differentiates between a

¹Code will be released upon acceptance of the paper.

user's *latent* and *expressed* opinion and uses a similar Hawkes process as in the CP model to model message intensity. SLANT requires fine-grained network information as training data; conversely, our approach requires only opinion volumes and is applicable in situations when network information is unavailable. OMM addresses the weaknesses mentioned above by proposing a two-tier approach, where the first tier models the dynamics of attention volume. In contrast, the second tier operates in a fixed-size setup, and the growth of one opinion leads to the shrinking of all others.

2 PRELIMINARIES

We introduce two classes of models that form the foundation of our approach: (1) the discrete-time Hawkes process [3], a model of event counts that display self-exciting behavior, and (2) the market share attraction model [7], a model from marketing literature that uncovers the latent competitive structure of a set of brands and the effects of a set of marketing instruments on brand market shares.

2.1 Discrete-time Hawkes Process

The discrete-time Hawkes Process (DTHP)[3] is the discrete-time analogue of the popular self-exciting Hawkes process [17], where instead of modeling the occurrence of events given by $t \in \mathbb{R}^+$, we model the count $N(t)$ of events on $[t-1, t)$ for $t \in \mathbb{N}$.

The DTHP is fully characterized by the conditional intensity function $\lambda(t)$, defined as the expected number of events that occur at time point t , conditioned on the history $H_{t-1} = \{N(s) | s < t\}$. For a DTHP, $\lambda(t)$ is given by

$$\lambda(t) = \mathbb{E}[N(t) | H_{t-1}] = \mu + \sum_{s < t} \alpha \cdot f(t-s) \cdot N(s), \quad (1)$$

where μ is the baseline count of events, α determines the level of self-excitation and is the expected number of events produced by a single event [36], and $f(t)$ is the triggering kernel, which controls the influence of the past events on the present. We specify $f(t)$ with the geometric probability mass function,

$$f(t) = \theta(1-\theta)^{t-1}, t \in \mathbb{N}, \quad (2)$$

the discrete-time analogue of the exponential distribution [3].

Since $\lambda(t)$ only provides the conditional mean of $N(t)$, one still has to specify a probability mass function for the event count $N(t)$. Following Browning et al. [3], we set $N(t) \sim \text{Poi}(\lambda(t))$.

Given a dataset of event counts $\{n_t | t \in \{1, \dots, T\}\}$, with n_t counting the number of events on $[t-1, t)$, one can determine the best-fitting DTHP parameters $\{\mu, \alpha, \theta\}$ by maximizing the log-likelihood function:

$$\mathcal{L}(\mu, \alpha, \theta | n_1 \dots n_T) \propto \sum_{t=1}^T \left[n_t \log \left(\mu + \alpha \sum_{s < t} n_s \theta (1-\theta)^{t-s-1} \right) - \left(\mu + \alpha \sum_{s < t} n_s \theta (1-\theta)^{t-s-1} \right) \right]. \quad (3)$$

2.2 Market Share Attraction Model

In marketing literature, *market share attraction models* (MSAMs) [7] model the competitive structure of a set of M brands in the same product category, predict their market shares, and evaluate

how a set of marketing instruments affects resulting market shares. We ultimately aim to cast opinions as brands and interventions as marketing instruments.

MSAMs assume that the market share s_i of brand $i \in \{1 \dots M\}$ is proportional to consumers' attraction \mathcal{A}_i towards brand i :

$$s_i = \frac{\mathcal{A}_i}{\sum_{m=1}^M \mathcal{A}_m} \in [0, 1]. \quad (4)$$

Brand i 's attraction \mathcal{A}_i is typically modeled as a parametric function of a set of K marketing instruments $\{X_{ki}\}_{k=1}^K \in \mathbb{R}^K$, where X_{ki} gives the value of the k^{th} marketing instrument for brand i . Typical examples of marketing instruments are the price of the product, ad spend, and distribution efforts.

A common specification of the attraction model is the multinomial logit (MNL) model given by

$$\mathcal{A}_i = \exp \left(\beta_i + \sum_{k=1}^K \sum_{j=1}^M \gamma_{kij} X_{kj} \right), \quad (5)$$

where β_i measures the inherent attraction of brand i and $\gamma_{kij} \in \mathbb{R}$ measures the effect of brand j 's k^{th} marketing instrument on brand i 's attraction. Whether γ_{kij} is positive (negative) is indicative of the excitatory (inhibiting) relationship from brand j to brand i through marketing instrument X_{kj} .

MSAMs are interpreted via the model elasticity $e(s_i, X_{kj})$, the ratio of the percent change in the market share s_i given a percent change in the k^{th} marketing instrument of brand j . That is,

$$e(s_i, X_{kj}) = \frac{\partial s_i / s_i}{\partial X_{kj} / X_{kj}} = \frac{\partial s_i}{\partial X_{kj}} \cdot \frac{X_{kj}}{s_i}. \quad (6)$$

The elasticity $e(s_i, X_{kj})$ captures the overall effect of brand j 's marketing instrument X_{kj} on brand i 's market share s_i : both the *direct effect* of X_{kj} on s_i , controlled by γ_{kij} , and the *indirect effect* of X_{kj} on s_i through its effect on the attraction of other brands $\{j \neq i\}$. An elasticity of $e(s_i, X_{kj}) = 0.1$ means that a 1% increase in X_{kj} corresponds to a 0.1% increase in s_i . Given a marketing instrument X_k , the elasticities $\{e(s_i, X_{kj})\}_{ij}$ form a matrix summarizing the cooperative-competitive interactions in the brand ecosystem.

3 MODEL

In Section 3.1, we develop a two-tier model of the opinion ecosystem. The first tier models the total size of the opinion attention market on multiple online platforms. The second tier models the market share of opinions on each platform.

In Section 3.2, we present an algorithm to sample opinion volumes from a fitted model and introduce a two-tier optimization scheme for parameter estimation.

3.1 Formulation

OMM consists of two tiers; the first tier, which we call the *opinion volume model*, tracks the size of the opinion attention market, while the second tier, the *opinion share model*, tracks the market shares of the different opinions.

Opinion volume model. We first model the total volume of attention. Consider P social media platforms on which users interact and post their opinions. Let $N^P(t)$ be the number of opinionated

posts on platform $p \in \{1, \dots, P\}$ on day $t \in \mathbb{N}$. We model $\{N^p(t)\}_p$ as a P -dimensional DTHP with conditional intensity $\{\lambda^p(t)\}_p$,

$$\lambda^p(t) = \mu^p \cdot S(t) + \sum_{q=1}^P \sum_{s < t} \alpha^{pq} \cdot f(t-s) \cdot N^q(s). \quad (7)$$

In contrast to Eq. (1), we use a time-varying exogenous signal $S(t)$, which accounts for the baseline volume of events of exogenous origin. The signal $S(t)$ accounts for natural tendencies and events (i.e., epidemics, elections) and typically cannot be controlled. We introduce a scaling term μ^p for each platform p such that $\mu^p \cdot S(t)$ represents the exogenous opinion count for platform p on day t .

Since online platforms are not siloed and have significant user overlap, we allow the P social media platforms to interact via intra- and inter-platform excitation. The parameter $\alpha^{pq} > 0$ sets the level of intra-platform excitation (for $p = q$) and inter-platform excitation (for $p \neq q$); and f is defined as in Eq. (2). Lastly, we set $N^p(t) \sim \text{Poi}(\lambda^p(t))$.

Opinion share model. With the size of the opinion attention market estimated in the first tier, the second tier models the market shares of the opinions in each platform. Given the limited attention market size, opinions compete for attention within each platform.

Suppose that there are M different opinions. We set $n_i^p(t)$ to be the number of opinionated posts conveying opinion i on platform p on day t , and $\lambda_i^p(t)$ to be its conditional intensity. We relate $\lambda_i^p(t)$ to $\lambda^p(t)$ in Eq. (7) by introducing the market share $s_i^p(t)$ and setting

$$\lambda_i^p(t) = \lambda^p(t) \cdot s_i^p(t). \quad (8)$$

Similar to Eq. (4), we define $s_i^p(t)$ using the attraction $\mathcal{A}_i^p(t)$,

$$s_i^p(t) = \frac{\mathcal{A}_i^p(t)}{\sum_{j=1}^M \mathcal{A}_j^p(t)}, \quad (9)$$

where, inspired by the MNL form in Eq. (5), we define attraction

$$\mathcal{A}_i^p(t) = \exp \mathcal{T}_i^p(t). \quad (10)$$

where $\mathcal{T}_i^p(t)$ depends on *interventions* and *endogenous* dynamics,

$$\mathcal{T}_i^p(t) = \underbrace{\sum_{k=1}^K \gamma_{ik}^p \cdot \bar{X}_k(s)}_{\text{interventions}} + \underbrace{\sum_{q=1}^P \sum_{j=1}^M \beta_{ij}^{pq} \cdot \lambda^q(t|j)}_{\text{endogenous}}, \quad \text{and} \quad (11)$$

$$\bar{X}_k(s) = \sum_{s < t} f(t-s) \cdot X_k(s).$$

To influence the opinion market share distribution on each platform, we introduce a set of K positive interventions $\{X_k(t)\}_k$. In contrast to $S(t)$ in Eq. (7), the interventions $\{X_k(t)\}_k$ affect the opinion ecosystem by modifying the opinion market shares, not the attention market size. The parameter $\gamma_{ik}^p \in \mathbb{R}$ measures the direct effect of the k^{th} intervention on the market share of opinion i on platform p . If γ_{ik}^p is positive (negative), then $X_k(t)$ reinforces (inhibits) opinion i on platform p .

For the endogenous part of Eq. (11), we use the conditional intensity $\lambda^p(t|j)$, which models the dynamics of opinion j independent

of other opinions. That is,

$$\lambda^p(t|j) = \mu_j^p \cdot S(t) + \sum_{q=1}^P \sum_{s < t} \alpha^{pq} \cdot f(t-s) \cdot N_j^q(s), \quad (12)$$

where $\mu^p = \sum_{j=1}^M \mu_j^p$. Intuitively, $\lambda^q(t|j)$ indicates the prevalence of opinion j on platform q . $\beta_{ij}^{pq} \in \mathbb{R}$ captures the direct effect that opinion j on platform q has on the market share of opinion i on platform p . Similar to γ_{ik}^p , we allow β_{ij}^{pq} to be positive (negative), representing a reinforcing (inhibiting) relationship from opinion j to i on platform q and p , respectively.

3.2 Simulation and Estimation

In this section, we present algorithms to (1) simulate opinion volumes from a fitted model and (2) estimate model parameters from a dataset of opinion volumes.

Simulation. Suppose we are given the opinion volume $n_{i,0}^p$ on day $t = 0$ for each platform p and opinion i , such that $n_t^p = \sum_i n_{i,t}^p$. We generate samples from the OMM by looping the following steps over $t \in \{1, \dots, T\}$ and each platform p and opinion i .

- (1) Compute $\lambda_i^p(t) = \lambda^p(t| \cup_{q,s < t} \{n_s^q\}) \cdot s_i^p(t| \cup_{q,j,s < t} \{n_{j,s}^q\})$.
- (2) Draw a sample $n_{i,t}^p \sim \text{Poi}(\lambda_i^p(t))$.

Estimation. Over the observation period $t \in \{1, \dots, T\}$, assume that we observe the exogenous signal $S(t)$, the K interventions $\{X_k(t)\}_k$, and the number $n_{i,t}^p$ of posts conveying opinion i on platform p for each i and p . Our goal is to estimate the parameter set $\Theta = \{\mu_j^p, \alpha^{pq}, \theta, \gamma_{ik}^p, \beta_{ij}^{pq}\}$.

The structure of our two-tier model naturally allows us to cast parameter optimization as a two-tier optimization problem. Let $\Theta_1 = \{\mu^p, \alpha^{pq}, \theta\}$. The key observation here is that the first-tier parameter set Θ_1 can be estimated using only the opinion volume model in Eq. (7), independent of the opinion share model in Eq. (11). By optimizing the likelihood $\mathcal{L}_1(\Theta_1 | \{n_{i,t}^p\}_{p,t})$ on the platform-level volumes $\{n_{i,t}^p\}_{p,t}$, one can obtain an estimate $\hat{\Theta}_1$ of Θ_1 .

The second-tier parameter set $\Theta_2 = \{\mu_j^p, \gamma_{ik}^p, \beta_{ij}^{pq}\}$ can be obtained by freezing $\hat{\Theta}_1$ and optimizing the likelihood $\mathcal{L}_2(\Theta_2 | \hat{\Theta}_1, \{n_{i,t}^p\}_{i,p,t})$ on the opinion volumes $\{n_{i,t}^p\}_{i,p,t}$. We summarize the parameter estimation task with the two-step procedure below.

- (1) Given $\{n_{i,t}^p\}_{p,t}$, find $\hat{\Theta}_1 = \Theta_1$ that maximizes

$$\mathcal{L}_1(\Theta_1 | \{n_{i,t}^p\}_{p,t}) = \sum_{t=1}^T \sum_{p=1}^P \left[n_{i,t}^p \log \lambda^p(t) - \lambda^p(t) \right]. \quad (13)$$

- (2) Given $\{n_{i,t}^p\}_{i,p,t}$ and $\hat{\Theta}_1$, find $\hat{\Theta}_2 = \Theta_2$ that maximizes

$$\mathcal{L}_2(\Theta_2 | \hat{\Theta}_1, \{n_{i,t}^p\}_{i,p,t}) = \sum_{i,p,t} \left[n_{i,t}^p (\log \lambda^p(t) \cdot s_i^p(t)) - (\lambda^p(t) \cdot s_i^p(t)) \right]. \quad (14)$$

Our estimated parameter set can be collected as $\hat{\Theta} = \hat{\Theta}_1 \cup \hat{\Theta}_2$.

The likelihoods $\mathcal{L}_1(\cdot)$ and $\mathcal{L}_2(\cdot)$ and the gradients $\partial_{\Theta_1} \mathcal{L}_1(\cdot)$ and $\partial_{\Theta_2} \mathcal{L}_2(\cdot)$ are derived in the online appendix [1].

Lastly, one can also fit the OMM on multiple realizations of event volumes. Given n_{samples} realizations, one can define the joint likelihood as the sum of likelihoods over the set of realizations, and

optimize the joint likelihood with the procedure detailed above. More details are provided in the online appendix [1].

4 LEARNING WITH SYNTHETIC DATA

In this section, we consider the task of parameter estimation with synthetic data. First, we discuss our experimental setup and the synthetic dataset. Next, we show that parameter recovery error decreases and stabilizes as we increase the training time T and the number of samples $n_{samples}$.

Experimental setup. For our test, we set $P = M = K = 2$. We set $\mu_1^1 = 15$, $\mu_2^1 = 5$, $\mu_1^2 = 5$, $\mu_2^2 = 20$, $\theta = 0.5$, and draw $\alpha^{pq} \sim \text{Unif}(0, 0.5)$, $\beta_{ij}^{pq} \sim \text{Unif}(0, 0.1)$ and $\gamma_{ik}^p \sim \text{Unif}(0, 0.1)$. For our exogenous signals, we set $S(t) = 1$, $X_1(t) = 5 \sin(0.1x) + 5$, and $X_2(t) = 10 \sin(0.05x + 1.25) + 10$.

We construct our synthetic dataset by using the simulation algorithm in Section 3.2 to obtain 400 samples of opinion volumes $\{n_{i,t}^p\}_{i,p,t}$ for $t \in \{1, \dots, T = 300\}$. We partition the 400 samples into 20 groups, where each group of $n_{samples} = 20$ samples is used as input to the joint fitting procedure using the likelihoods in Eq. (13) and Eq. (14). With this procedure, we obtain 20 sets of estimates for each parameter in $\Theta = \{\mu_j^p, \alpha^{pq}, \theta, \gamma_{ik}^p, \beta_{ij}^{pq}\}$.

Model evaluation. We compute the root mean-squared error (RMSE) of our estimated $\hat{\Theta} = \{\hat{\mu}_j^p, \hat{\alpha}^{pq}, \hat{\theta}, \hat{\gamma}_{ik}^p, \hat{\beta}_{ij}^{pq}\}$ with respect to the true Θ . We report the average RMSE per parameter type separately, where the average is taken over the components of the matrix or tensor corresponding to the parameter type.

In Fig. 2(a) we see that training on a longer timeframe leads to lower RMSE for both $\hat{\alpha}^{pq}$ and $\hat{\beta}_{ij}^{pq}$, as well as better model fit as measured by the likelihood \mathcal{L}_2 in Eq. (14). Results for $\hat{\mu}_j^p$, $\hat{\theta}$ and $\hat{\gamma}_{ik}^p$, and on varying $n_{samples}$ are shown in the online appendix [1].

In Fig. 2(b) we plot the distribution of the difference between our estimates and the true values. We recover first-tier parameters $\{\mu_j^p, \alpha^{pq}\}$ well, as evidenced by our mean estimates coinciding with the true values. For the second-tier parameters $\{\gamma_{ik}^p, \beta_{ij}^{pq}\}$ we observe slight overestimation.

5 REAL-WORLD FAR-RIGHT OPINIONS

In this section, we test OMM on a dataset of discussions annotated with moderate and far-right opinions. First, we introduce the *Bushfire Opinions dataset*, the exogenous signal $S(t)$ and the positive intervention $X(t)$ (Section 5.1). Second, we evaluate OMM's performance in predicting volumes and market share distributions of opinions (Section 5.2). Lastly, we interpret the obtained model elasticities to understand opinion relations, and perform what-if scenarios to understand the effect of the intervention (Section 5.3).

5.1 Dataset and far-right opinion labeling

Dataset. We construct the *Bushfire Opinions dataset*, containing 90 days of Twitter and Facebook discussions about bushfires and climate change. The Facebook postings are a subset of the *SocialSense* dataset [23]; we select the posts & comments relating to bushfires and climate change (the *SocialSense* also contains discussions around COVID-19). These were collected using CrowdTangle by crawling public far-right Australian Facebook groups, identified via

a digital ethnographic study (see [23] and the online appendix [1] for more details). We build the Twitter discussions using the Twitter Academic v2 API; we collect tweets emitted between November 1, 2019 to January 29, 2020 that mention bushfire keywords such as *bushfire*, *arson*, *australiaburns*, or *climate hoax* (see full list in the online appendix [1]). We use the AWS Location Service to geocode users based on their free-text location and description fields and filter only for tweets from Australian users.

Moderate and far-right opinion labeling. We use the textual opinion classifiers developed by Kong et al. [23] to label Facebook and Twitter postings; we select the following most prevalent six opinions, covering 95% of Twitter and 81% of Facebook postings:

- (0) Greens policies are the cause of the Australian bushfires.
- (1) Mainstream media cannot be trusted.
- (2) Climate change crisis is not real / is a UN hoax.
- (3) Australian bushfires and climate change are not related.
- (4) Australian bushfires were caused by random arsonists.
- (5) Bushfires are a normal summer occurrence in Australia.

Furthermore, we deploy the far-right stance detector introduced by Ram and Rizoiu [30] – which leverages a textual homophily measurement to quantify the similarity between Twitter users and known far-right activists. An opinion occurrence is labeled as *far-right* if the posting agrees with the opinion (denoted as +), or *moderate* if the posting disagrees with the opinion (-). We represent our opinion set as $\{(i-, i+)\mid i \in \{0, \dots, 5\}\}$. We obtain 74,461 tweets and 7,974 Facebook postings labeled with $M = 12$ stanced opinions. We aggregate posting volumes into hourly counts, yielding $T = 2,160$ time points over the 90 days from Nov 1, 2019, to Jan 29, 2020.

Exogenous signal S and intervention X. The exogenous signal $S(t)$ (Eq. (7)) modulates the total size of the attention market in the first tier of OMM. We use the 5-day rolling average of the Google Search Trends in Australia for the terms *bushfire+climate change* normalized to a maximum value of 1. Google Trends captures the baseline interest on the topic and acts as a proxy for offline events (like the actual bushfires and government measures).

The intervention $\{X_k(t)\}$ modulates the market share of far-right and moderate opinions. We consider the coverage by news from traditional publishers as the single tested instrument ($K = 1$). We extract the set of news outlets from the Reputable News Index (RNIX) [24]; we query Factiva to obtain the daily news volumes of these outlets. Finally, we subtract the Google Trends signal from the news volume. Let $\text{news}(t)$ be the daily volume of reputable news. We compute $X(t)$ as $X(t) = \text{news}(t) - \frac{\max_t \text{news}(t)}{\max_t S(t)} S(t)$. $X(t)$ is interpreted as the extent to which media over- or under-reports the bushfire crisis relative to the public's attention.

Numerical considerations. To improve model fit and numerical stability, we implement three augmentations to the proposed model and estimation method in Section 3, outlined below and fully detailed in the online appendix [1]. First, we modify the expression for the attraction $\mathcal{A}_i^p(t)$ in Eq. (9) to prevent numerical overflow and underflow. Second, we add a regularization term in the second-tier optimization problem in Section 3.2 to improve estimation of Θ_2 . Third, we apply log-scaling on $\lambda^q(t|j)$ and standardization on both $\lambda^q(t|j)$ and $\bar{X}_k(s)$ in Eq. (11) to solve scaling issues.

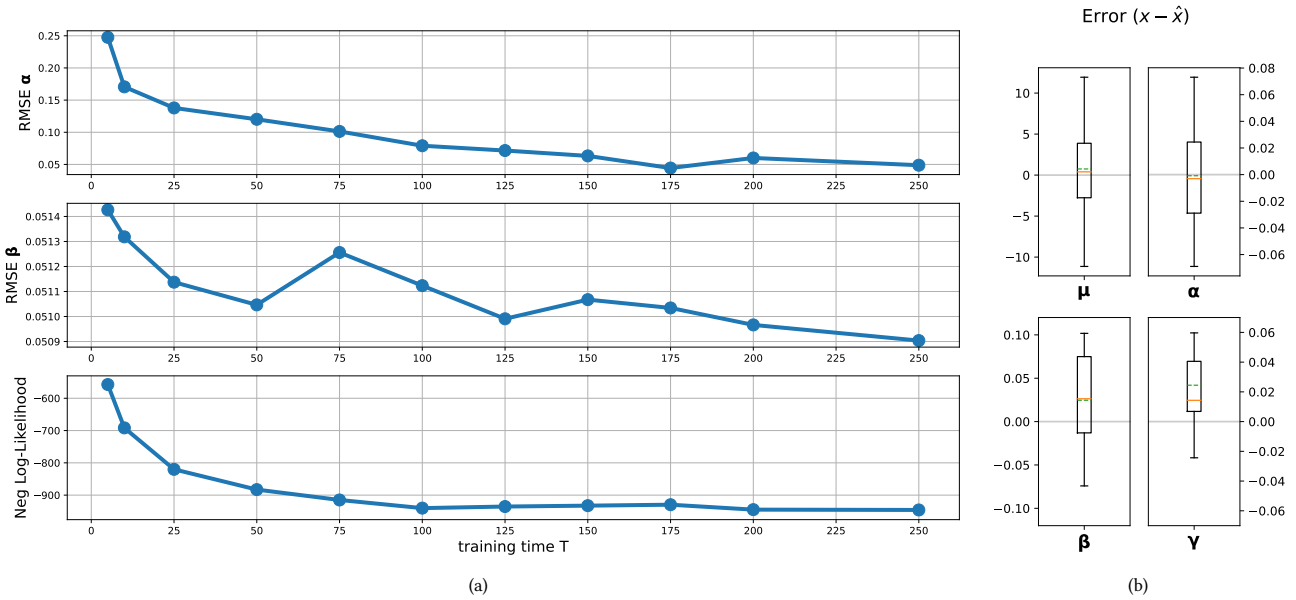


Figure 2: Parameter recovery results on synthetic data. In (a), we show the convergence of the RMSE of the α and β estimates and the negative log-likelihood as we increase the training time T . In (b), we show the difference between our estimates for $\{\mu, \alpha, \beta, \gamma\}$ and the true values. Dashed green lines and orange lines are the mean and median values, respectively.

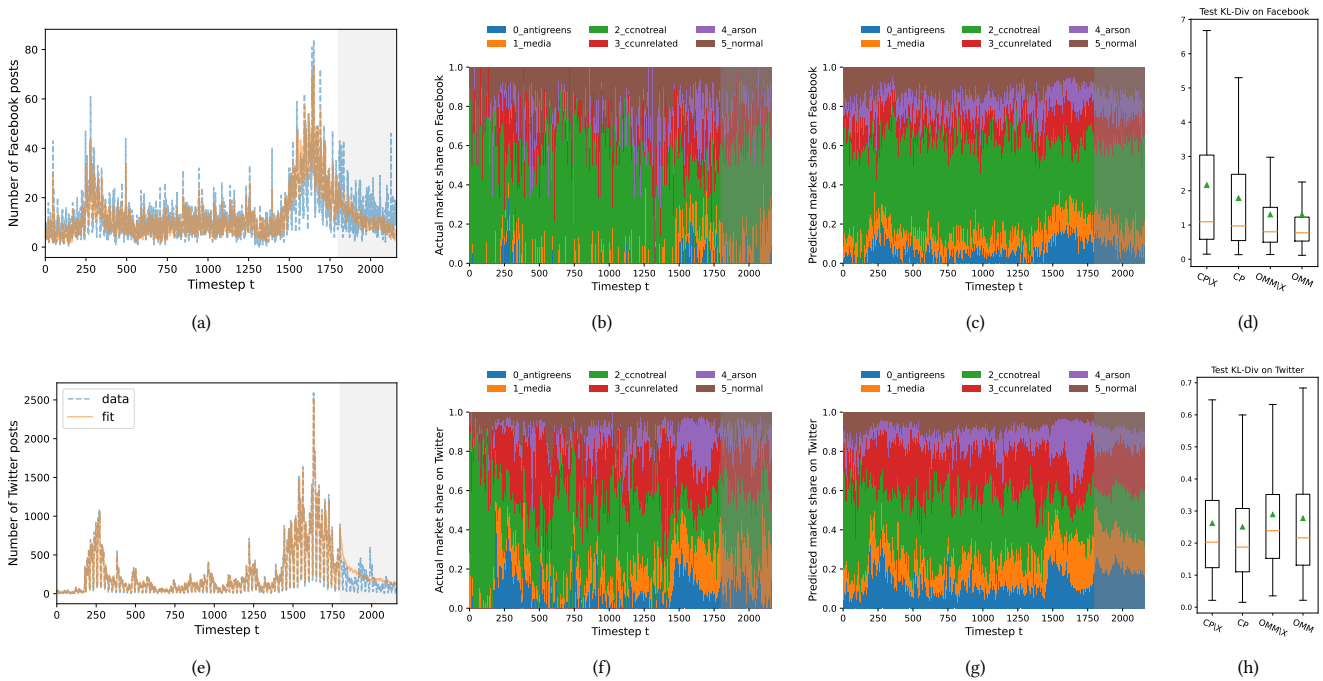


Figure 3: Evaluating the OMM on the Bushfire Opinions dataset. We train OMM on the first 1800 timesteps and predict on timesteps 1801 to 2160 (shaded area). We present results for Facebook and Twitter, respectively. We aggregate the far-right and moderate versions of opinions in plots b, c, f & g. (a & d) Actual (dashed blue lines) vs. fitted/predicted (orange lines) opinion volumes; (b & f) Actual opinion market share; (c & g) Fitted/predicted opinion market shares; and (d & h) KL-divergence on the evaluation set for the CP baselines and OMM with and without media coverage $X(t)$.

5.2 Predictive evaluation

Model setup. We evaluate OMM using a temporal holdout strategy: following prior literature [31], we fit OMM on $\mathcal{T}_{obs} = \{1, \dots, 1800\}$, where time is in hours (i.e., days 1-75 of our period of interest), and evaluate performance on $\mathcal{T}_{pred} = \{1801, \dots, 2160\}$ (i.e. days 76-90).

We consider two tasks: (1) opinion volume prediction and (2) opinion distribution prediction. For opinion volume prediction, we predict the total volume of opinionated posts on Facebook and Twitter during the evaluation period. We measure performance using the symmetric mean absolute percentage error (SMAPE) of our predicted volumes $\{\bar{n}_t^p | t \in \mathcal{T}_{pred}\}$ on platform p relative to the actual volumes $\{n_t^p | t \in \mathcal{T}_{pred}\}$, given by

$$\text{SMAPE}(p) = \frac{100\%}{360} \sum_{t=1801}^{2160} \frac{|\bar{n}_t^p - n_t^p|}{|\bar{n}_t^p| + |n_t^p|}. \quad (15)$$

The predicted opinion volumes $\{\bar{n}_t^p\}$, are obtained using the simulation algorithm in Section 3.2. We (1) condition on $\{n_{i,t}^p | t \in \mathcal{T}_{obs}\}$, (2) run the algorithm forward to obtain samples of $\{n_{i,t}^p\}$ on \mathcal{T}_{pred} , then (3) sum over opinion types $\{i\}$ to get predicted opinion volumes $n_t^p = \sum_i n_{i,t}^p$. We repeat $R = 5$ times, and average the results over the samples to get predicted opinion volumes $\{\bar{n}_t^p | t \in \mathcal{T}_{pred}\}$.

For opinion distribution prediction, we predict opinion market shares $\{s_{i,t}^p\}$ for each platform p on the evaluation period. We evaluate using the KL-divergence of our predicted market shares $\{\bar{s}_{i,t}^p | t \in \mathcal{T}_{pred}\}$ (obtained similar to $\{\bar{n}_t^p\}$ described above) relative to the actual market shares $\{s_{i,t}^p | t \in \mathcal{T}_{pred}\}$.

$$\text{KL}^p(t) = \sum_{i=1}^M s_{i,t}^p \log \frac{\bar{s}_{i,t}^p}{s_{i,t}^p}. \quad (16)$$

We compare OMM with two discretized versions of the Competing Products (CP) model [35] – the current state of the art model in product share modeling, covered in related works: with and without the intervention $X(t)$. Both versions account for the exogenous signal $S(t)$. We compare opinion volume prediction (first tier) with CP without $X(t)$; we compare the market share prediction (second tier) against both flavors of CP.

Predictive evaluation results. Figs. 3(a) and 3(e) show the observed (blue line) and modeled (orange line) volumes of opinions for Facebook and Twitter, respectively. The modeled line shows the fitting during the training period and the prediction during the testing period (hashed area). For both platforms, OMM (SMAPE(FB) = 22.65%, SMAPE(TW) = 35.61%), outperforms the CP baseline (SMAPE(FB) = 24.80%, SMAPE(TW) = 37.14%).

We show the observed (Fig. 3(b)) and fitted/predicted (Fig. 3(c)) market shares for Facebook (Figs. 3(f) and 3(g) for Twitter). We see that OMM captures the trend in the opinion distributions on both platforms. In Figs. 3(d) and 3(h), we show the $\text{KL}^p(t)$ divergence between observed and predicted opinion distributions, for Facebook and Twitter, respectively. We test the effectiveness of the intervention by predicting with and without $X(t)$. We make several observations. First, performances are better for Twitter than Facebook ($\text{KL}^{TW}(t) < \text{KL}^{FB}(t)$), likely due to Facebook having lower opinion counts than Twitter. Second, OMM consistently outperforms

CP on Facebook (Fig. 3(d)), and has comparable performances on Twitter (Fig. 3(h)). This is because CP does not have a notion of limited total attention, and due to higher volumes of postings on Twitter, CP pays more attention to Twitter, leading to low performance on Facebook. Lastly, models with $X(t)$ outperform versions without $X(t)$; this suggests that mainstream media is effective in shaping the opinion ecosystem.

Uncovering opinions interactions. To study interactions between opinions and interventions, we calculate the opinion share model elasticities (see Eq. (6)) with respect to the intervention $\bar{X}(s)$ and the endogenous volume $\lambda^p(t|j)$ (see Eq. (11)). The endogenous elasticities $e(s_i^p(t), \lambda^q(t|j))$ quantify the competition-cooperation interactions across opinions. The intervention elasticities $e(s_i^p(t), \bar{X}(t))$ quantify the sensitivity of opinion market shares to mainstream media coverage $X(t)$. We derive the elasticities in the online appendix [1]. Elasticities are time-varying, and Fig. 4 reports their averages over time.

First, we study the intra-platform reinforcement (top-left and bottom-right matrices in Fig. 4(a)). We see that Facebook and Twitter exhibit different behaviors. OMM detects little interaction among opinions within Facebook since the dataset was collected from far-right groups with limited interaction with users of the opposing side. For Twitter, we have two key observations. First, there is strong self-reinforcement for opinions on Twitter (i.e., the main diagonal), indicative of the echo chamber effect. Second, there is significant cross-reinforcement among far-right sympathizers and opponents (i.e., the diagonals on the upper-right & lower-left submatrices), indicative of exchanges or arguments between the opposing camps.

How to effectively suppress far-right opinions. The above implies that confrontation is not the most effective method to suppress far-right opinions, as it has the potential to backfire by bringing even more attention to them. A more effective method is boosting related counter-arguments; for instance, to suppress "Climate change is not real" (2+) on Twitter, OMM indicates to promote "Greens are not the cause of the bushfires" (0-), and "Australian bushfires were not caused by random arsonists" (4-). Boosting the opposite argument, i.e., "Climate change is real" (2-), would backfire. The opinion "Bushfires are a normal summer occurrence in Australia" (5+) shows a different behavior: it reinforces moderate opinions (except for 4-, the "Arson" opinion) and inhibits far-right opinions. In particular, the "Bushfires are normal" opinion (5+) appears to trigger "Climate change is real" (2-), probably due to the diametric nature of these opinions. The effect of 5+ on 2- holds across platforms from Twitter to Facebook (upper right matrix); additionally, "Bushfires are normal" (5+) also reinforces "Climate change is not real" (2+), probably due to the overlap of their views.

Cross-platform reinforcement is generally weak due to the Facebook far-right groups acting as a filter bubble. Apart from the effect of "Bushfires are normal" (5+) (see above), there is little cross-reinforcement among opinions from Twitter to Facebook. In the bottom left matrix, we see that moderate opinions on Facebook have a small reinforcing effect on "Bushfires were caused by arson" (4+) and "Bushfires are normal" (5+) opinions on Twitter.

Intervention elasticities $e(s_i^p(t), \bar{X}(t))$. We see that news has very small elasticities on Facebook, suggesting that mainstream media coverage does not penetrate far-right Facebook groups. For

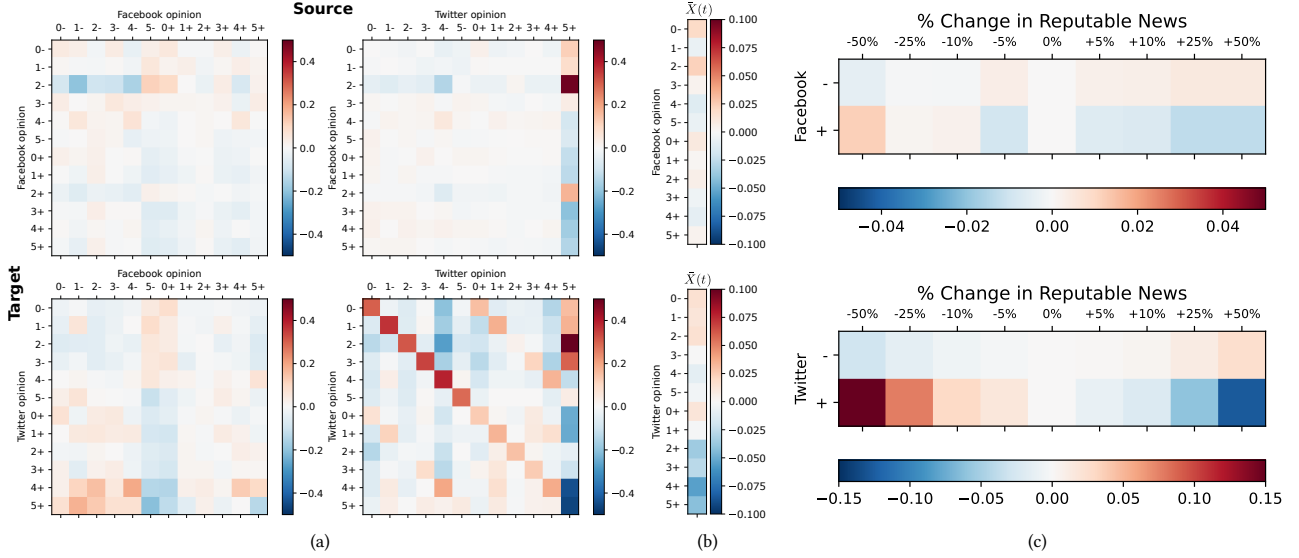


Figure 4: Interpretability of OMM. (a) Time-averaged endogenous elasticities $e(s_i^p(t), \lambda^q(t|j))$. Elasticities have direction and should be read from column (source) to row (target), both for the platform and within each color matrix. For example, the bottom right matrix corresponds to influences from Twitter to Twitter; the cell $\{4+, 4-\}$ ({row, column}) is the influence of opinion 4- on 4+, here positive and large meaning that 4- has a strong reinforcing effect on 4+. (b) The intervention elasticities $e(s_i^p(t), \bar{X}(t))$ of the intervention on each opinion, on each platform. (c) We modulate the volume of reputable news from -50% to 50% of the mean volume and simulate OMM forward to see the percentage change in the market shares of far-right (+) and moderate (-) opinions on Facebook (top row) and Twitter (bottom row). For brevity, we aggregate the six (+) and six (-) opinions.

Twitter, we see a more consistent and stronger effect – mainstream media coverage inhibits the majority of the far-right opinions and reinforces the majority of the moderate opinions. Across opinions, we see that on both platforms, "Arson caused bushfires" (4+) was the most responsive to the intervention. At the same time, "Mainstream media cannot be trusted" (1+) was the least, which is intuitive, as the evaluated intervention is the mainstream media.

5.3 Does the media suppress far-right opinions?

The intervention $X(t)$ can lead to delayed effects in the opinion ecosystem due to the dependency structure of OMM. However, model elasticities only inform us of the *instantaneous* effect on the opinion market shares. We perform a what-if exercise in which we vary the size of the intervention and we sample synthetic outcomes to investigate the long-term effects of media coverage on the opinion ecosystem.

What-if setup. We modulate the reputable news signal $X(t)$ as $X^{(r)}(t) = X(t) + r \cdot \mu_X \cdot \mathbb{1}_{(t > 1800)}$, where $\mathbb{1}_{(\cdot)}$ is the indicator function and μ_X is the mean volume of $X(t)$ on \mathcal{T}_{obs} . The parameter r controls the percentage increase ($r > 0$) or decrease ($r < 0$) in media coverage beyond the change point $t = 1800$; $r = 0$ is the original $X(t)$ (see Section 5.1). We run OMM with $X^{(r)}(t)$ for various r . We quantify the effect of the modulated intervention as the average percent change (relative to $r = 0$) in the opinion market shares after the change point, i.e., \mathcal{T}_{pred} .

More news leads to less far-right opinions. Fig. 4(c) shows the average percent changes in the market share of far-right and moderate opinions for various r over 50 simulations. For both Facebook and Twitter, larger media coverage leads to more significant suppression of far-right opinions. The effect of the news on Facebook is significantly less than on Twitter: for a 50% increase in the level of reputable news, we see a 15% decrease in the far-right market share on Twitter but just a $< 4\%$ decrease on Facebook. As a result, increasing the media coverage appears to be a viable strategy to suppress far-right opinions on Twitter. However, the far-right public groups on Facebook behave as almost perfect filter bubbles in which reputable news has little penetration. We also see that media coverage has a modest strengthening effect on the market share of moderate opinions.

6 CONCLUSION

This work introduces the Opinion Market Model, a novel two-tier model of the dynamics of the online opinion ecosystem. The first tier models the size of the attention market, and the second tier models opinions competing or cooperating for limited public attention under the influence of positive interventions. We develop algorithms to simulate and estimate OMM and show convergence of our learning scheme using a synthetic dataset. We demonstrate real-world applicability by testing OMM on a dataset of Facebook and Twitter discussions containing moderate and far-right opinions about bushfires and climate change [23]. We show OMM predicts opinion market shares better than the state-of-the-art baseline [35]

and uncovers latent competitive and cooperative interactions across opinions: self-reinforcement attributable to the echo chamber effect and interactions between far-right sympathizers and opponents. Lastly, we show through simulation that mainstream media coverage is an effective positive intervention to stem far-right opinion.

Future work. The flexibility of OMM allows us to test alternative specifications of the positive intervention $X(t)$ in the bushfire case study. We can consider both mainstream $X_1(t)$ and alternative media coverage $X_2(t)$, or media coverage specific to each opinion, i.e., $X_{k_i}(t)$, for $i \in \{1, \dots, M\}$. Fitting OMM to these alternative specifications gives us more fine-grained interactions between opinions and interventions.

REFERENCES

- [1] 2022. Appendix: Opinion Market Model: Stemming Far-Right Opinion Spread using Positive Interventions. <https://bit.ly/3AgiZyA>.
- [2] Joan Balcells and Albert Padró-Solanet. 2016. Tweeting on Catalonia's independence: The dynamics of political discussion and group polarisation. *Media Studies* 7, 14 (2016).
- [3] Raiha Browning, Deborah Sulem, Kerrie Mengersen, Vincent Rivoirard, and Judith Rousseau. 2021. Simple discrete-time self-exciting models can describe complex dynamic processes: A case study of COVID-19. *PLoS ONE* 16 (2021).
- [4] Uthsav Chitra and Christopher Musco. 2020. Analyzing the Impact of Filter Bubbles on Social Network Polarization. In *Proceedings of the 13th International Conference on Web Search and Data Mining* (Houston, TX, USA) (WSDM '20). New York, NY, USA. <https://doi.org/10.1145/3336191.3371825>
- [5] Matteo Cinelli, Gianmarco De Francisci Morales, Alessandro Galeazzi, Walter Quattrociocchi, and Michele Starnini. 2021. The echo chamber effect on social media. *Proceedings of the National Academy of Sciences* 118, 9 (2021), e2023301118.
- [6] Katherine Clayton, Spencer Blair, Jonathan A Busam, Samuel Forstner, John Glance, Guy Green, Anna Kawata, Akhila Kovvuri, Jonathan Martin, Evan Morgan, et al. 2020. Real solutions for fake news? Measuring the effectiveness of general warnings and fact-check tags in reducing belief in false stories on social media. *Political Behavior* 42, 4 (2020), 1073–1095.
- [7] Lee G. Cooper. 1993. Chapter 6 Market-share models. In *Marketing*. Handbooks in Operations Research and Management Science, Vol. 5. Elsevier, 259–314.
- [8] Matthew Costello, James Hawdon, Thomas Ratliff, and Tyler Grantham. 2016. Who views online extremism? Individual attributes leading to exposure. *Computers in Human Behavior* 63 (2016), 311–320.
- [9] Abir De, Isabel Valera, Niloy Ganguly, Sourangshu Bhattacharya, and Manuel Gomez-Rodriguez. 2016. Learning and Forecasting Opinion Dynamics in Social Networks. In *Proceedings of the 30th International Conference on Neural Information Processing Systems* (Barcelona, Spain) (NIPS'16). Curran Associates Inc., Red Hook, NY, USA, 397–405.
- [10] Sachi Edwards. 2017. Hate Speech Bigotry and Oppression of Hindus through the Internet. *Digital Hinduism: Dharma and Discourse in the Age of New Media* 111 (2017).
- [11] Seth Flaxman, Sharad Goel, and Justin M Rao. 2016. Filter bubbles, echo chambers, and online news consumption. *Public opinion quarterly* 80, S1 (2016), 298–320.
- [12] Kiran Garimella, Gianmarco De Francisci Morales, Aristides Gionis, and Michael Mathioudakis. 2017. Reducing Controversy by Connecting Opposing Views. In *Proceedings of the Tenth ACM International Conference on Web Search and Data Mining* (Cambridge, United Kingdom) (WSDM '17). Association for Computing Machinery, New York, NY, USA, 81–90. <https://doi.org/10.1145/3018661.3018703>
- [13] Samrat Gupta, Gaurav Jain, and Amit Anand Tiwari. 2022. Polarised social media discourse during COVID-19 pandemic: evidence from YouTube. *Behaviour & Information Technology* (2022), 1–22.
- [14] Gulizar Hacıyakupoglu, Jennifer Yang Hui, VS Suguna, Dymples Leong, and Muhammad Faizal Bin Abdul Rahman. 2018. Countering fake news: A survey of recent global initiatives. (2018).
- [15] Shahrzad Haddadan, Cristina Menghini, Matteo Riondato, and Eli Upfal. 2021. RePBuLiK: Reducing Polarized Bubble Radius with Link Insertions. In *Proceedings of the 14th ACM International Conference on Web Search and Data Mining* (Virtual Event, Israel) (WSDM '21). Association for Computing Machinery, New York, NY, USA, 139–147. <https://doi.org/10.1145/3437963.3441825>
- [16] Ghayda Hassan, Sébastien Brouillette-Alarie, S raphin Alava, Divina Frau-Meigs, Lysiane Lavoie, Arber Fetiu, Wynnpaul Varela, Evgueni Borokhovski, Vivek Venkatesh, C cile Rousseau, et al. 2018. Exposure to extremist online content could lead to violent radicalization: A systematic review of empirical evidence. *International journal of developmental science* 12, 1-2 (2018), 71–88.
- [17] Alan G. Hawkes. 1971. Spectra of Some Self-Exciting and Mutually Exciting Point Processes. *Biometrika* 58, 1 (1971), 83–90. <http://www.jstor.org/stable/2334319>
- [18] Minna Horowitz, Stephen Cushion, Marius Dragomir, Sergio Guti rrez Manj n, and Mervi Pantti. 2022. A framework for assessing the role of public service media organizations in countering disinformation. *Digital Journalism* 10, 5 (2022), 843–865.
- [19] Nicholas K Iammarino and Thomas W O'Rourke. 2018. The challenge of alternative facts and the rise of misinformation in the digital age: Responsibilities and opportunities for health promotion and education. *American journal of health education* 49, 4 (2018), 201–205.
- [20] Sam Jackson. 2019. The double-edged sword of banning extremists from social media. (2019).
- [21] Brent Kitchens, Steven L Johnson, and Peter Gray. 2020. Understanding Echo Chambers and Filter Bubbles: The Impact of Social Media on Diversification and Partisan Shifts in News Consumption. *MIS Quarterly* 44, 4 (2020).
- [22] Ilkka Koiranen, Aki Koivula, Sanna Malinen, and Teo Keipi. 2022. Undercurrents of echo chambers and flame wars: party political correlates of social media behavior. *Journal of Information Technology & Politics* 19, 2 (2022), 197–213.
- [23] Quyu Kong, Emily Booth, Francesco Bailo, Amelia Johns, and Marian-Andrei Rizoiu. 2022. Slipping to the Extreme: A Mixed Method to Explain How Extreme Opinions Infiltrate Online Discussions. In *AAAI International Conference on Web and Social Media*, Vol. 16. 524–535. arXiv:2109.00302 <http://arxiv.org/abs/2109.00302https://ojs.aaai.org/index.php/ICWSM/article/view/19312>
- [24] Quyu Kong, Marian-Andrei Rizoiu, and Lexing Xie. 2020. Describing and predicting online items with reshare cascades via dual mixture self-exciting processes. In *Proceedings of the 29th ACM International Conference on Information & Knowledge Management*. 645–654.
- [25] Seth A. Myers and Jure Leskovec. 2012. Clash of the contagions: Cooperation and competition in information diffusion. *Proceedings - IEEE International Conference on Data Mining, ICDM* (2012).
- [26] Elmie Nekmat. 2020. Nudge effect of fact-check alerts: source influence and media skepticism on sharing of news misinformation in social media. *Social Media+ Society* 6, 1 (2020), 2056305119897322.
- [27] Shruti Phadke and Tanushree Mitra. 2020. Many faced hate: A cross platform study of content framing and information sharing by online hate groups. In *Proceedings of the 2020 CHI Conference on Human Factors in Computing Systems*.
- [28] Ethan Porter and Thomas J Wood. 2021. Fact checks actually work, even on Facebook. But not enough people see them. *The Washington Post* (2021), NA–NA.
- [29] Ga l Poux-M dard, Julien Velcin, and Sabine Loudcher. 2021. Information Interaction Profile of Choice Adoption. In *Machine Learning and Knowledge Discovery in Databases. Research Track*, Nuria Oliver, Fernando P rez-Cruz, Stefan Kramer, Jesse Read, and Jose A. Lozano (Eds.). Vol. 12977. Springer International Publishing, Cham, 103–118. https://doi.org/10.1007/978-3-030-86523-8_7 Series Title: Lecture Notes in Computer Science.
- [30] Rohit Ram and Marian-Andrei Rizoiu. 2022. You are what you browse: A robust framework for uncovering political ideology. (aug 2022). arXiv:2208.04097 <http://arxiv.org/abs/2208.04097>
- [31] Marian-Andrei Rizoiu, Lexing Xie, Scott Sanner, Manuel Cebrian, Honglin Yu, and Pascal Van Hentenryck. 2017. Expecting to be HIP: Hawkes Intensity Processes for Social Media Popularity. In *Proceedings of the 26th International Conference on World Wide Web*. International World Wide Web Conferences Steering Committee, Republic and Canton of Geneva, Switzerland, 735–744. arXiv:1602.06033
- [32] Kai Shu, Suhang Wang, and Huan Liu. 2019. Beyond News Contents: The Role of Social Context for Fake News Detection. In *Proceedings of the Twelfth ACM International Conference on Web Search and Data Mining* (Melbourne VIC, Australia) (WSDM '19). Association for Computing Machinery, New York, NY, USA, 312–320. <https://doi.org/10.1145/3289600.3290994>
- [33] Dominic Spohr. 2017. Fake news and ideological polarization: Filter bubbles and selective exposure on social media. *Business information review* 34, 3 (2017).
- [34] Utkarsh Upadhyay, Abir De, Aasish Pappu, and Manuel Gomez-Rodriguez. 2019. On the Complexity of Opinions and Online Discussions. In *Proceedings of the Twelfth ACM International Conference on Web Search and Data Mining* (Melbourne VIC, Australia) (WSDM '19). Association for Computing Machinery.
- [35] Isabel Valera and Manuel Gomez-Rodriguez. 2015. Modeling Adoption and Usage of Competing Products. In *2015 IEEE International Conference on Data Mining*. IEEE, Atlantic City, NJ, USA, 409–418. <https://doi.org/10.1109/ICDM.2015.40>
- [36] Gentry White, Michael D. Porter, and Lorraine Mazerolle. 2013. Terrorism Risk, Resilience and Volatility: A Comparison of Terrorism Patterns in Three Southeast Asian Countries. *Journal of Quantitative Criminology* 29, 2 (June 2013), 295–320. <https://doi.org/10.1007/s10940-012-9181-y>
- [37] Joe Whittaker. 2020. Online Echo Chambers and Violent Extremism. *The Digital Age, Cyber Space, and Social Media: The Challenges of Security & Radicalization* (2020), 129–150.
- [38] Michael Wolfowicz, David Weisburd, and Badi Hasisi. 2021. Examining the interactive effects of the filter bubble and the echo chamber on radicalization. *Journal of Experimental Criminology* (2021), 1–23.
- [39] Liang Wu and Huan Liu. 2018. Tracing Fake-News Footprints: Characterizing Social Media Messages by How They Propagate. In *Proceedings of the Eleventh ACM International Conference on Web Search and Data Mining* (Marina Del Rey, CA, USA) (WSDM '18). Association for Computing Machinery, New York, NY,

- USA, 637–645. <https://doi.org/10.1145/3159652.3159677>
- [40] Siqu Wu, Marian-Andrei Rizoiu, and Lexing Xie. 2019. Estimating Attention Flow in Online Video Networks. *Proceedings of the ACM on Human-Computer Interaction* 3, CSCW (nov 2019), 1–25. <https://doi.org/10.1145/3359285>
- [41] Xiaofei Xu, Ke Deng, and Xiuzhen Zhang. 2022. Identifying Cost-Effective Debunkers for Multi-Stage Fake News Mitigation Campaigns. In *Proceedings of the Fifteenth ACM International Conference on Web Search and Data Mining (Virtual Event, AZ, USA) (WSDM '22)*. Association for Computing Machinery, New York, NY, USA, 1206–1214. <https://doi.org/10.1145/3488560.3498457>
- [42] Greyson K Young. 2022. How much is too much: the difficulties of social media content moderation. *Information & Communications Technology Law* 31, 1 (2022), 1–16.
- [43] Ali Zarezade, Ali Khodadadi, Mehrdad Farajtabar, Hamid R. Rabiee, and Hongyuan Zha. 2017. Correlated cascades: Compete or cooperate. *31st AAAI Conference on Artificial Intelligence, AAAI 2017 (2017)*, 238–244. eprint: 1510.00936.
- [44] Rui Zhang, Christian Walder, and Marian-Andrei Rizoiu. 2020. Variational Inference for Sparse Gaussian Process Modulated Hawkes Process. *Proceedings of the AAAI Conference on Artificial Intelligence* 34, 04 (apr 2020). arXiv:1905.10496

This document accompanies the submission *Opinion Market Model: Stemming Far-Right Opinion Spread using Positive Interventions*. The information in this document complements the submission and is presented here for completeness reasons. It is not required to understand the main paper or reproduce the results.

A MODEL LIKELIHOOD AND GRADIENTS

A.1 Likelihood formulation

Likelihood function $\mathcal{L}_1(\Theta_1|\{n_t^p\}_{p,t})$, where $\Theta_1 = \{\mu^p, \alpha^{pq}, \theta\}$. The log-likelihood function can be derived by

$$\begin{aligned} & \mathcal{L}_1(\Theta_1|\{n_t^p\}_{p,t}) \\ &= \log \mathbb{P} \left\{ \bigcup_{t=1}^T \bigcup_{p=1}^P [N^p(t) = n_t^p] \right\} \\ &= \sum_{t=1}^T \sum_{p=1}^P \log \mathbb{P} \{N^p(t) = n_t^p\} \\ &= \sum_{t=1}^T \sum_{p=1}^P \log \left[\frac{e^{-\lambda^p(t)} \lambda^p(t)^{n_t^p}}{n_t^p!} \right] \\ &\propto \sum_{t=1}^T \sum_{p=1}^P \left[n_t^p \log \lambda^p(t) - \lambda^p(t) \right] \end{aligned} \quad (17)$$

Likelihood function $\mathcal{L}_2(\Theta_2|\Theta_1, \{n_{i,t}^p\}_{i,p,t})$, where $\Theta_2 = \{\mu_j^p, \gamma_{ik}^p, \beta_{ij}^{pq}\}$.

Instead of estimating the parameters $\mu_j^p \in \mathbb{R}$, we can estimate the normalized parameters $\hat{\mu}_j^p \in [0, 1]$, where $\mu_j^p = \mu^p \cdot \hat{\mu}_j^p$. Given that the magnitudes of γ_{ik}^p and β_{ij}^{pq} are typically less than one, estimating normalized parameters $\hat{\mu}_j^p$ instead of μ_j^p avoids scaling problems. Hence, we optimize for $\Theta_2 = \{\hat{\mu}_j^p, \gamma_{ik}^p, \beta_{ij}^{pq}\}$.

$$\begin{aligned} & \mathcal{L}_2(\Theta_2|\Theta_1, \{n_{i,t}^p\}_{i,p,t}) \\ &= \log \mathbb{P} \left\{ \bigcup_{t=1}^T \bigcup_{p=1}^P \bigcup_{i=1}^M [N_i^p(t) = n_{i,t}^p] \right\} \\ &= \sum_{t=1}^T \sum_{p=1}^P \sum_{i=1}^M \log \mathbb{P} \{N_i^p(t) = n_{i,t}^p\} \\ &= \sum_{t=1}^T \sum_{p=1}^P \sum_{i=1}^M \log \left[\frac{e^{-\lambda_i^p(t)} \lambda_i^p(t)^{n_{i,t}^p}}{n_{i,t}^p!} \right] \\ &\propto \sum_{t=1}^T \sum_{p=1}^P \sum_{i=1}^M \left[n_{i,t}^p \log \lambda_i^p(t) - \lambda_i^p(t) \right] \\ &= \sum_{t=1}^T \sum_{p=1}^P \sum_{i=1}^M \left[n_{i,t}^p \log(\lambda^p(t) \cdot s_i^p(t)) - (\lambda^p(t) \cdot s_i^p(t)) \right] \\ &= \sum_{t=1}^T \sum_{p=1}^P \sum_{i=1}^M \left[n_{i,t}^p (\log \lambda^p(t) + \log s_i^p(t)) - (\lambda^p(t) \cdot s_i^p(t)) \right] \end{aligned} \quad (18)$$

A.2 Gradients

Gradient $\partial_{\Theta_1} \mathcal{L}_1(\Theta_1|\{n_t^p\}_{p,t})$. Differentiating Eq. (17), we get

$$\partial_{\Theta_1} \mathcal{L}_1(\Theta_1|\{n_t^p\}_{p,t}) = \sum_{t=1}^T \sum_{p=1}^P \frac{\partial_{\Theta_1} \lambda^p(t)}{\lambda^p(t)} \cdot \left[n_t^p - \lambda^p(t) \right],$$

where

$$\partial_{\mu^{pq}} \lambda^p(t) = \delta_{pq}$$

$$\partial_{\alpha^{qr}} \lambda^p(t) = \delta_{pq} \cdot \sum_{s < t} f(t-s) \cdot N^r(s)$$

$$\partial_{\theta} \lambda^p(t) = \sum_{q=1}^P \sum_{s < t} \alpha^{pq} \cdot \partial_{\theta} f(t-s) \cdot N^q(s)$$

$$\partial_{\theta} f(t) = (1-\theta)^{t-2} [1-\theta t].$$

Gradient $\partial_{\Theta_2} \mathcal{L}_2(\Theta_2|\Theta_1, \{n_{i,t}^p\}_{i,p,t})$. Differentiating Eq. (18), we get

$$\begin{aligned} \partial_{\Theta_2} \mathcal{L}_2(\Theta_2|\Theta_1, \{n_{i,t}^p\}_{i,p,t}) & \sum_{t=1}^T \sum_{p=1}^P \sum_{i=1}^M \left[\frac{\partial_{\Theta_2} \lambda^p(t)}{\lambda^p(t)} + \frac{\partial_{\Theta_2} s_i^p(t)}{s_i^p(t)} \right] \\ & \cdot \left[n_{i,t}^p - \lambda^p(t) \cdot s_i^p(t) \right], \end{aligned} \quad (19)$$

where upon differentiating Eq. (9) and Eq. (10) we have

$$\partial_{\Theta_2} s_i^p(t) = \frac{\left[\sum_j \mathcal{A}_j^p(t) \right] \partial_{\Theta_2} \mathcal{A}_i^p(t) - \mathcal{A}_i^p(t) \left[\sum_j \partial_{\Theta_2} \mathcal{A}_j^p(t) \right]}{\left[\sum_j \mathcal{A}_j^p(t) \right]^2}, \quad (20)$$

and

$$\partial_{\Theta_2} \mathcal{A}_i^p(t) = \mathcal{A}_i^p(t) \cdot \partial_{\Theta_2} \mathcal{T}_i^p(t). \quad (21)$$

Plugging in Eq. (21) into Eq. (20), we get

$$\begin{aligned} \partial_{\Theta_2} s_i^p(t) &= \frac{\left[\sum_j \mathcal{A}_j^p(t) \right] \mathcal{A}_i^p(t) \cdot \partial_{\Theta_2} \mathcal{T}_i^p(t) - \mathcal{A}_i^p(t) \left[\sum_j \mathcal{A}_j^p(t) \cdot \partial_{\Theta_2} \mathcal{T}_j^p(t) \right]}{\left[\sum_j \mathcal{A}_j^p(t) \right]^2} \\ &= \frac{\mathcal{A}_i^p(t) \left[\sum_j \mathcal{A}_j^p(t) \cdot \partial_{\Theta_2} \mathcal{T}_i^p(t) \right] - \left[\sum_j \mathcal{A}_j^p(t) \cdot \partial_{\Theta_2} \mathcal{T}_j^p(t) \right]}{\left[\sum_j \mathcal{A}_j^p(t) \right]^2} \\ &= \frac{\mathcal{A}_i^p(t)}{\left[\sum_j \mathcal{A}_j^p(t) \right]^2} \cdot \sum_j \mathcal{A}_j^p(t) \cdot \left[\partial_{\Theta_2} \mathcal{T}_i^p(t) - \partial_{\Theta_2} \mathcal{T}_j^p(t) \right] \\ &= s_i^p(t) \cdot \sum_j s_j^p(t) \cdot \left[\partial_{\Theta_2} \mathcal{T}_i^p(t) - \partial_{\Theta_2} \mathcal{T}_j^p(t) \right], \end{aligned}$$

and so

$$\begin{aligned} \frac{\partial_{\Theta_2} s_i^p(t)}{s_i^p(t)} &= \sum_j s_j^p(t) \cdot \left[\partial_{\Theta_2} \mathcal{T}_i^p(t) - \partial_{\Theta_2} \mathcal{T}_j^p(t) \right] \\ &= \partial_{\Theta_2} \mathcal{T}_i^p(t) - \sum_j s_j^p(t) \cdot \partial_{\Theta_2} \mathcal{T}_j^p(t) \\ &= \sum_j (\delta_{ij} - s_j^p(t)) \cdot \partial_{\Theta_2} \mathcal{T}_j^p(t) \end{aligned} \quad (22)$$

Plugging in Eq. (22) into Eq. (19), we have

$$\begin{aligned} \partial_{\Theta_2} \mathcal{L}_2(\Theta_2 | \Theta_1, \{n_{i,t}^p\}_{i,p,t}) &= \sum_{t=1}^T \sum_{p=1}^P \sum_{i=1}^M \left[\frac{\partial_{\Theta_2} \lambda^p(t)}{\lambda^p(t)} \right. \\ &\left. + \sum_{j=1}^M (\delta_{ij} - s_j^p(t)) \cdot \partial_{\Theta_2} \mathcal{T}_j^p(t) \right] \cdot \left[n_{i,t}^p - \lambda^p(t) \cdot s_i^p(t) \right], \quad (23) \end{aligned}$$

where

$$\begin{aligned} \partial_{\mu_j^q} \lambda^p(t) &= \delta_{pq} \\ \partial_{\gamma_{ik}^q} \lambda^p(t) &= 0 \\ \partial_{\beta_{ij}^{pq}} \lambda^p(t) &= 0 \\ \partial_{\mu_j^q} \mathcal{T}_i^p(t) &= \beta_{ij}^{pq} \\ \partial_{\gamma_{jk}^q} \mathcal{T}_i^p(t) &= \delta_{ij} \delta_{qp} \cdot \sum_{s < t} f(t-s) \cdot X_k(s) \\ \partial_{\beta_{jk}^{qr}} \mathcal{T}_i^p(t) &= \delta_{ij} \delta_{qp} \cdot \lambda^r(t|k) \end{aligned}$$

A.3 Fitting on multiple samples.

Suppose that we are given $n_{samples}$ samples to fit the OMM.

Let $\mathcal{S} = \left\{ \{n_{i,t}^p\}_{i,p,t}^s \mid s \in \{1, \dots, n_{samples}\} \right\}$. One can define the joint likelihood over \mathcal{S} as the average likelihood over the $n_{samples}$ samples. That is,

$$\begin{aligned} \mathcal{L}_1(\Theta_1 | \mathcal{S}) &= \frac{1}{n_{samples}} \sum_{s=1}^{n_{samples}} \mathcal{L}_1(\Theta_1 | \{n_{i,t}^p\}_{i,p,t}^s) \\ \mathcal{L}_2(\Theta_2 | \Theta_1, \mathcal{S}) &= \frac{1}{n_{samples}} \sum_{s=1}^{n_{samples}} \mathcal{L}_2(\Theta_2 | \Theta_1, \{n_{i,t}^p\}_{i,p,t}^s). \end{aligned}$$

where $\mathcal{L}_1(\cdot)$ and $\mathcal{L}_2(\cdot)$ are defined in Eq. (13) and Eq. (14), respectively. Parameter optimization proceeds in the same setup as the two-step procedure detailed in Section 3.2.

B ADDITIONAL RESULTS FOR SYNTHETIC DATA

In Fig. 5 we show the behavior of the RMSE for μ , θ , β as we increase the training time T . Error stabilises and the model converges as we increase T . In Fig. 6 we show behavior of the RMSE of our parameters as we vary the number of samples in the joint fit $n_{samples}$. Increasing the number of samples improves performance on the first-tier parameters μ , θ and α , but does not have a strong improvement on the second-tier parameters β and γ . Increasing $n_{samples}$ stabilizes the likelihood of the fit.

C NUMERICAL CONSIDERATIONS

C.1 Stability of the softmax function

In Eq. (10), the tendency $\mathcal{T}_i^p(t)$ is unconstrained, and it can take both really large or really small numbers, which leads to numerical overflow and underflow in Eq. (9). To remedy this, instead of Eq. (10) we use

$$\tilde{\mathcal{A}}_i^p(t) = \exp \left[\mathcal{T}_i^p(t) - \max_{k \in \{1, \dots, M\}} \mathcal{T}_k^p(t) \right],$$

which does not affect market share calculations since

$$s_i^p(t) = \frac{\mathcal{A}_i^p(t)}{\sum_{j=1}^M \mathcal{A}_j^p(t)} = \frac{\tilde{\mathcal{A}}_i^p(t)}{\sum_{j=1}^M \tilde{\mathcal{A}}_j^p(t)}.$$

Gradient and elasticity calculations are unaffected when we use $\tilde{\mathcal{A}}_i^p(t)$ instead of $\mathcal{A}_i^p(t)$.

C.2 Opinion share model regularization

Fitting the opinion share model to data involves estimation of $\Theta_2 = \{\hat{\mu}_j^p, \gamma_{ik}^p, \beta_{ij}^{pq}\}$, a total of $P \times M + P \times M \times K + P^2 \times M^2$ parameters. Given the high dimensionality of this space, we add L2 regularization term to the likelihood function. Instead of Eq. (14), we solve

$$\hat{\Theta}_2 = \arg \min_{\Theta_2} \left[-\mathcal{L}_2(\Theta_2 | \hat{\Theta}_1, \{n_{i,t}^p\}_{i,p,t}) + \lambda \|\Theta_2\|_2 \right],$$

where λ is a regularization parameter we set to 0.1.

Likelihood gradients become

$$-\partial_{\Theta_2} \mathcal{L}_2(\Theta_2 | \hat{\Theta}_1, \{n_{i,t}^p\}_{i,p,t}) + \Theta_2 \cdot \lambda.$$

C.3 Transformations on $\lambda^q(t|j)$ and $\bar{X}_k(s)$ in $\mathcal{T}_i^p(t)$

We perform two transformations on $\lambda^q(t|j)$ and $\bar{X}_k(s)$ in Eq. (11) to improve model fit.

First, it was observed that $\lambda^q(t|j)$ has a skewed distribution over time. The skewness is problematic since we estimate a time-independent linear parameter β_{ij}^{pq} for the direct effect of $\lambda^q(\cdot|j)$ on $\mathcal{T}_i^p(t)$. To reduce the skewness of $\lambda^q(\cdot|j)$, we transform $\lambda^q(t|j)$ to $\log[\lambda^q(t|j) + 1]$, where we add 1 to avoid taking the logarithm of 0. Second, since $\mathcal{T}_i^p(t)$ is a linear combination of $\lambda^q(t|j)$ and $\bar{X}_k(t)$ terms, which could have totally different scales, we standardize these terms to bring them to a normalized scale. Let

$$\tilde{\lambda}^q(t|j) = \frac{\log[\lambda^q(t|j) + 1] - \text{mean}_s \log[n_{j,s}^q + 1]}{\text{std}_s \log[n_{j,s}^q + 1]},$$

$$\tilde{X}_k(t) = \frac{\bar{X}_k(t) - \text{mean}_s [\bar{X}_k(s)]}{\text{std}_s [\bar{X}_k(s)]}$$

where the mean and standard deviation are computed over the training period.

Instead of Eq. (11), we use the following form of the tendency:

$$\mathcal{T}_i^p(t) = \sum_{k=1}^K \gamma_k^p \cdot \tilde{X}_k(t) + \sum_{q=1}^P \sum_{j=1}^M \beta_{ij}^{pq} \cdot \tilde{\lambda}^q(t|j). \quad (24)$$

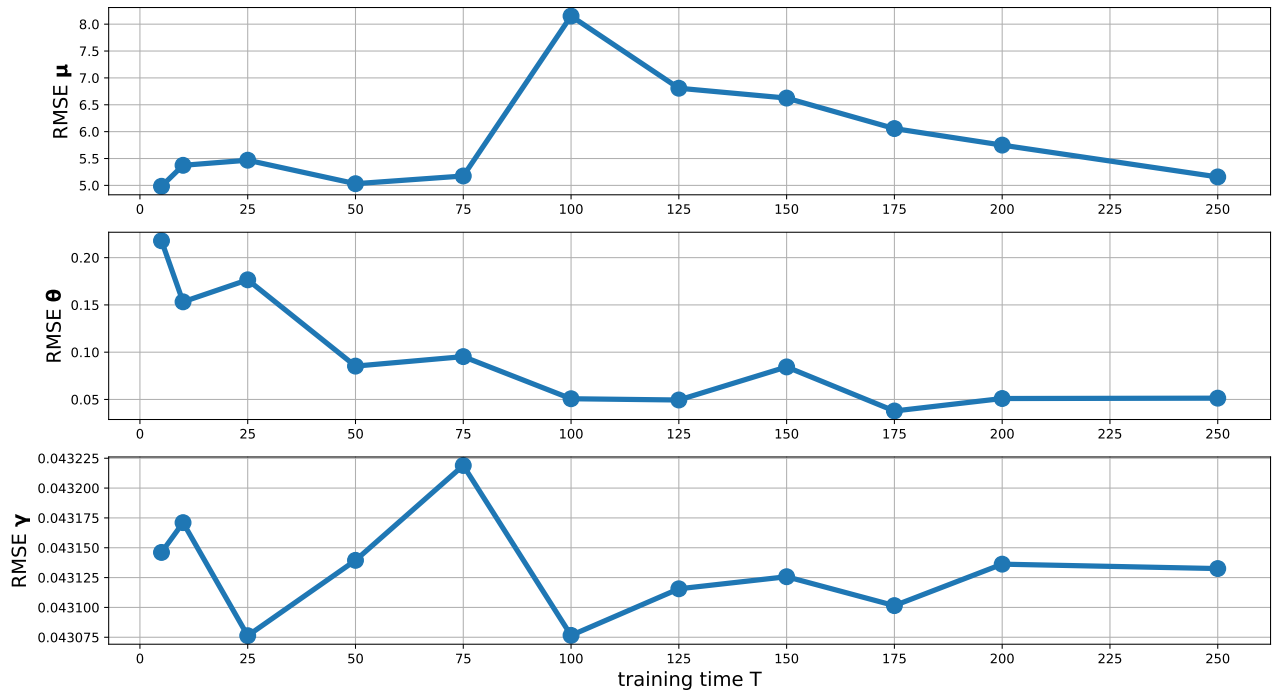


Figure 5: Additional results on synthetic data. We show the convergence of the RMSE of the μ, θ, β as we increase the training time T .

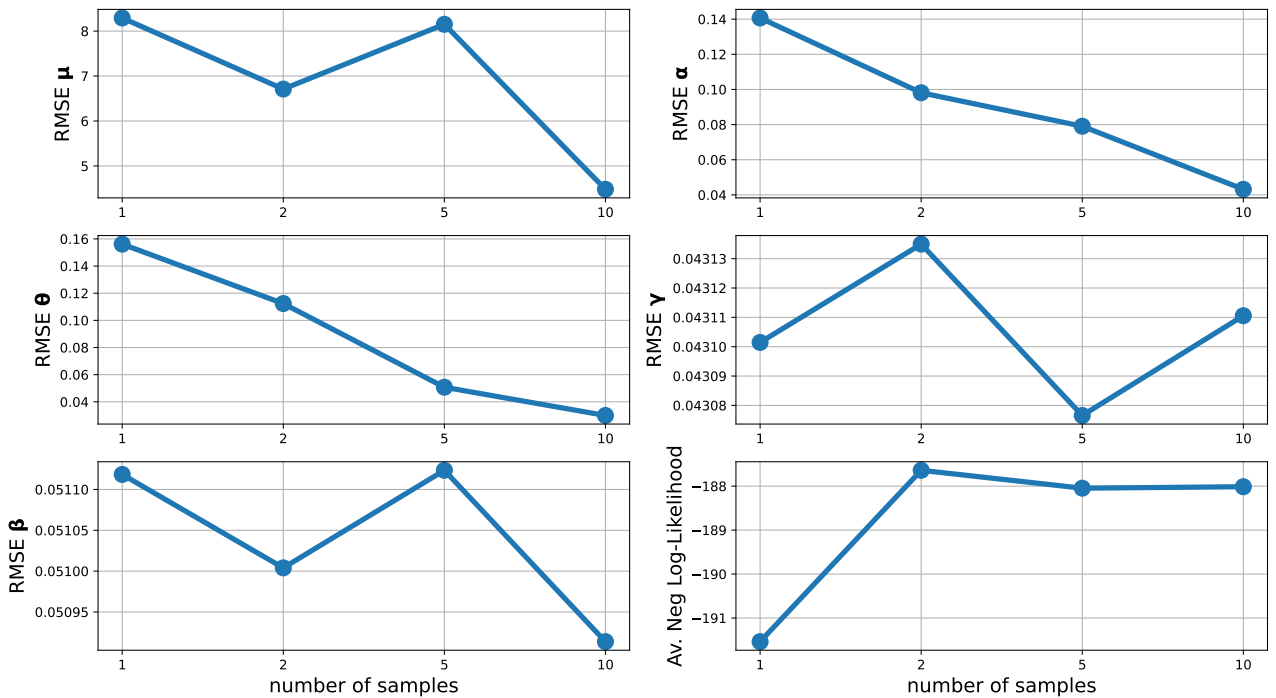


Figure 6: Additional results on synthetic data. We show the behavior of the RMSE of our parameter set and the average negative log likelihood as we vary the number of samples in the joint fit.

D MODEL ELASTICITIES

D.1 Endogenous elasticities $e(s_i^p(t), \lambda^q(t|j))$

Applying Eq. (6) on Eq. (9) and Eq. (24), we obtain the endogenous elasticities $e(s_i^p(t), \lambda^q(t|j))$ as follows:

$$\begin{aligned}
& e(s_i^p(t), \bar{X}_k(t)) \\
&= \frac{\partial \bar{X}_k(t)}{\partial s_i^p(t)} \cdot \frac{\bar{X}_k(t)}{s_i^p(t)} \\
&= \left\{ -\frac{\mathcal{A}_i^p(t)}{[\sum_j \mathcal{A}_j^p(t)]^2} \frac{\partial \bar{X}_k(t)}{\partial \bar{X}_k(t)} \sum_k \mathcal{A}_k^p(t) + \frac{\partial \bar{X}_k(t)}{\partial \bar{X}_k(t)} \frac{\mathcal{A}_i^p(t)}{\sum_j \mathcal{A}_j^p(t)} \right\} \cdot \frac{\bar{X}_k(t)}{s_i^p(t)} \\
&= \left\{ -\frac{s_i^p(t)}{\sum_k \mathcal{A}_k^p(t)} \sum_j \mathcal{A}_j^p(t) \frac{\gamma_{jk}^p}{\sigma_{X,k}} + \frac{\mathcal{A}_i^p(t)}{\sum_j \mathcal{A}_j^p(t)} \cdot \frac{\gamma_{ik}^p}{\sigma_{X,k}} \right\} \cdot \frac{\bar{X}_k(t)}{s_i^p(t)} \\
&= \left\{ -\frac{s_i^p(t)}{\sum_j \mathcal{A}_j^p(t)} \sum_j \mathcal{A}_j^p(t) \frac{\gamma_{jk}^p}{\sigma_{X,k}} + s_i^p(t) \cdot \frac{\gamma_{ik}^p}{\sigma_{X,k}} \right\} \cdot \frac{\bar{X}_k(t)}{s_i^p(t)} \\
&= \left\{ -s_i^p(t) \sum_j \left[\frac{\mathcal{A}_j^p(t)}{\sum_l \mathcal{A}_l^p(t)} \right] \frac{\gamma_{jk}^p}{\sigma_{X,k}} + s_i^p(t) \cdot \frac{\gamma_{ik}^p}{\sigma_{X,k}} \right\} \cdot \frac{\bar{X}_k(t)}{s_i^p(t)} \\
&= \left\{ -s_i^p(t) \sum_j s_j^p(t) \frac{\gamma_{jk}^p}{\sigma_{X,k}} + s_i^p(t) \cdot \frac{\gamma_{ik}^p}{\sigma_{X,k}} \right\} \cdot \frac{\bar{X}_k(t)}{s_i^p(t)} \\
&= \left\{ -\sum_j s_j^p(t) \frac{\gamma_{jk}^p}{\sigma_{X,k}} + \frac{\gamma_{ik}^p}{\sigma_{X,k}} \right\} \cdot \bar{X}_k(t) \\
&= \frac{\bar{X}_k(t)}{\sigma_{X,k}} \cdot \sum_j [\delta_{ij} - s_j^p(t)] \gamma_{jk}^p
\end{aligned}$$

D.2 Intervention elasticities $e(s_i^p(t), \bar{X}_k(t))$

Applying Eq. (6) on Eq. (9) and Eq. (24), we obtain the intervention elasticities $e(s_i^p(t), \bar{X}_k(t))$ as follows. Let

$$\phi_j^q(t) = \frac{1}{\text{std}_s \log [N_j^q(s) + 1]} \cdot \frac{1}{\lambda^q(t|j) + 1}.$$

Then we have:

$$\begin{aligned}
& e(s_i^p(t), \lambda^q(t|j)) \\
&= \frac{\partial \lambda^q(t|j)}{\partial s_i^p(t)} \cdot \frac{\lambda^q(t|j)}{s_i^p(t)} \\
&= \left\{ -\frac{\mathcal{A}_i^p(t)}{[\sum_k \mathcal{A}_k^p(t)]^2} \frac{\partial \lambda^q(t|j)}{\partial \lambda^q(t|j)} \sum_k \mathcal{A}_k^p(t) + \frac{\partial \lambda^q(t|j)}{\partial \lambda^q(t|j)} \frac{\mathcal{A}_i^p(t)}{\sum_k \mathcal{A}_k^p(t)} \right\} \cdot \frac{\lambda^q(t|j)}{s_i^p(t)} \\
&= \left\{ -\frac{s_i^p(t)}{\sum_k \mathcal{A}_k^p(t)} \sum_k \mathcal{A}_k^p(t) \frac{\beta_{kj}^{pq}}{\phi_j^q(t)} + \frac{\mathcal{A}_i^p(t)}{\sum_k \mathcal{A}_k^p(t)} \cdot \frac{\beta_{ij}^{pq}}{\phi_j^q(t)} \right\} \cdot \frac{\lambda^q(t|j)}{s_i^p(t)} \\
&= \left\{ -\frac{s_i^p(t)}{\sum_k \mathcal{A}_k^p(t)} \sum_k \mathcal{A}_k^p(t) \frac{\beta_{kj}^{pq}}{\phi_j^q(t)} + s_i^p(t) \cdot \frac{\beta_{ij}^{pq}}{\phi_j^q(t)} \right\} \cdot \frac{\lambda^q(t|j)}{s_i^p(t)} \\
&= \left\{ -s_i^p(t) \sum_k \left[\frac{\mathcal{A}_k^p(t)}{\sum_l \mathcal{A}_l^p(t)} \right] \frac{\beta_{kj}^{pq}}{\phi_j^q(t)} + s_i^p(t) \cdot \frac{\beta_{ij}^{pq}}{\phi_j^q(t)} \right\} \cdot \frac{\lambda^q(t|j)}{s_i^p(t)} \\
&= \left\{ -s_i^p(t) \sum_k s_k^p(t) \frac{\beta_{kj}^{pq}}{\phi_j^q(t)} + s_i^p(t) \cdot \frac{\beta_{ij}^{pq}}{\phi_j^q(t)} \right\} \cdot \frac{\lambda^q(t|j)}{s_i^p(t)} \\
&= \left\{ -\sum_k s_k^p(t) \frac{\beta_{kj}^{pq}}{\phi_j^q(t)} + \frac{\beta_{ij}^{pq}}{\phi_j^q(t)} \right\} \cdot \lambda^q(t|j) \\
&= \frac{\lambda^q(t|j)}{\phi_j^q(t)} \cdot \sum_k [\delta_{ki} - s_k^p(t)] \beta_{kj}^{pq}
\end{aligned}$$

E DATASET CONSTRUCTION

The *Bushfire Opinions dataset* consists of Twitter posts and Facebook posts & comments from Australian user accounts and pages expressing problematic opinions on climate change and the 2019-2020 Australian bushfire season during the 90-day period of November 1, 2019 to January 29, 2020.

The Bushfire Opinions dataset derives from the *SocialSense dataset* introduced in [23], which consists of user posts and comments from three major online social media platforms: Facebook, Twitter and Youtube. Postings included in the SocialSense were on two general topics – first, the Australian bushfires and climate change, and second, Covid-19 and vaccination – and expressed problematic opinions. In this work, we focus on Facebook/ Twitter and the Australian bushfires/ climate change topic. Postings were collected using Crowdtangle focused on a set of far-right Australian Facebook groups identified with a digital ethnographic study (for Facebook), the Twitter commercial API (for Twitter), and the Youtube API (for Youtube) using the following keywords as input: *bushfire*, *australian fires*, *arson*, *scottyfrommarketing*, *liarfromtheshiar*, *australiaburns*, *australiaburning*, *itsthegreensfault*, *backburning*, *back burning*, *climate change*, *climate emergency*, *climate hoax*, *climate crisis*, *climate action now*. It is important to point out that the Facebook sample is sourced predominantly from far-right groups, whereas the Twitter and Youtube are general scrapes. Two sets of augmentations were added to the postings: the *topic* and the *opinion* of the post, obtained using a set of topic and opinion classifiers trained in [23]. The set of opinions was constructed via a qualitative study.

A limitation of the original SocialSense dataset is that the Twitter dataset for the Australian bushfires/ climate change topic was scraped only from December 2019 to February 2020, which did not capture early opinion during the start of the bushfire crisis. To that end, we decided to resrape the Twitter dataset from November 1, 2019 to January 29, 2020 using the Twitter Academic v2 API and the same set of keywords. Since the Twitter Academic API does not allow querying based on user account location, we utilized AWS's Amazon Location Service to geocode users based on their free-text location and description fields and filtered only for tweets from Australian users. Finally, we applied the same set of topic and opinion classifiers to augment the Twitter data.

Once we aligned the Facebook dataset from SocialSense and the rescraped Twitter dataset on the target timeframe, we observed that 10 (out of 34) opinions account for most of the Twitter (95%) and Facebook (81%) postings. To limit the set of opinions in our analysis, we focus on six *opinions of interest* constructed by merging subsets of the 10 opinions, after which we then filter the Twitter and Facebook datasets on this set of opinions. We index the six opinions we consider as $\{0, 1, 2, 3, 4, 5\}$ and are shown below:

- (0) Greens influence and policy are the cause of the 2019-2020 Australian bushfires./ I am opposed to the policies of Greens political parties.
- (1) Mainstream media cannot be trusted.

- (2) Climate change crisis isn't real/ Climate change is a UN hoax/ Climate change is a scam to generate profit for the wealthy and powerful.
- (3) 2019-2020 Australian bushfires and climate change not related.
- (4) 2019-2020 Australian bushfires were caused by random arsonists.
- (5) Changes in the earth's climate are a natural, normal phenomenon/Bush fires are a normal summer occurrence for Australia.

Lastly, keeping in mind our goal of uncovering the interactions between sympathisers and opponents of the aforementioned problematic opinions, we furthermore differentiate whether the expressed opinion shows a *far-right* or *moderate* stance, which effectively splits our set of 6 opinions into 12 *stanced* opinions. For instance, the anti-Greens opinion (labeled 0) splits as far-right (labeled 0+) and moderate (labeled 0-). We represent our set of opinions as $\{(i-, i+)|i \in \{0, \dots, 5\}\}$. We leverage the far-right stance detector introduced by Ram and Rizoio [30] and apply it on each post of the aligned Facebook and Twitter dataset.

In summary, the *Bushfire Opinions dataset* consists of posts on $P = 2$ platforms: 474,461 on Twitter and 27,974 on Facebook, exhibiting $M = 12$ stanced opinions. For compatibility with our discrete-time model, we aggregate post volumes on Facebook and Twitter into hourly counts, yielding $T = 2,160$ time points over the 90-day period of November 1, 2019 to January 29, 2020.